A&A 518, L148 (2010)
DOI: 10.1051/0004-6361/201014701

Astronomy & Astrophysics
Special feature

Herschel: the first science highlights

Letter to the Editor

"TNOs are Cool": A survey of the trans-Neptunian region

III. Thermophysical properties of 90482 Orcus and 136472 Makemake⋆

T. L. Lim[1], J. Stansberry[2], T. G. Müller[3], M. Mueller[4], E. Lellouch[5], C. Kiss[6], P. Santos-Sanz[5], E. Vilenius[3], S. Protopapa[7], R. Moreno[5], A. Delsanti[5,8], R. Duffard[9], S. Fornasier[5,10], O. Groussin[8], A. W. Harris[11], F. Henry[5], J. Horner[12], P. Lacerda[13], M. Mommert[11], J. L. Ortiz[9], M. Rengel[7], A. Thirouin[9], D. Trilling[14], A. Barucci[5], J. Crovisier[5], A. Doressoundiram[5], E. Dotto[15], P. J. Gutiérrez Buenestado[9], O. Hainaut[16], P. Hartogh[7], D. Hestroffer[17], M. Kidger[18], L. Lara[9], B. M. Swinyard[1], and N. Thomas[19]
(Affiliations are available in the online edition)

Received 1 April 2010 / Accepted 12 May 2010

ABSTRACT

Context. The goal of the *Herschel* open time programme "*TNOs are Cool!*" is to derive the physical and thermal properties for a large sample of Centaurs, and trans-Neptunian objects (TNOs), including resonant, classical, detached and scattered disk objects.
Aims. Based on observations of two targets we tried (i) to optimise the SPIRE observing technique for faint (close to the background confusion noise), slowly moving targets; (ii) to test different thermal model techniques; (iii) to determine radiometric diameter and albedo values; (iv) to compare with *Spitzer* results whenever possible.
Methods. We obtained SPIRE photometry on two targets and PACS photometry on one of the targets.
Results. We present results for the two targets, (90482) Orcus and (136472) Makemake, observed with SPIRE and for one of those targets, Makemake, observed with PACS. We adopt $p_V = 0.27$ and $D = 850$ km as our best estimate of the albedo and diameter of Orcus using single terrain models. With two-terrain models for Makemake, the bright terrain is fitted by, $0.78 < p_V < 0.90$, and the dark terrain $0.02 < p_V < 0.12$, giving $1360 < D < 1480$ km.
Conclusions. A single terrain model was derived for Orcus through the SPIRE photometry combined with MIPS data. The Makemake data from MIPS, PACS and SPIRE combined are not compatible with a single terrain model, but can be modelled with a two-terrain fit. These science demonstration observations have shown that the scanning technique, which allows us to judge the influence of background structures, has proved to be a good basis for this key programme.

Key words. techniques: photometric – Kuiper belt objects: individual: 90482 Orcus – Kuiper belt objects: individual: 136472 Makemake – infrared: general – submillimeter: general

1. Introduction

The objects (136472) Makemake (formerly 2005 FY9) and (90482) Orcus (formerly 2004 DW) are among the largest trans-Neptunian objects (TNOs). Orcus has a diameter near 1000 km (Stansberry et al. 2008), and is one of the few binary TNOs in an orbit resonant with that of Neptune. Near-IR spectroscopy indicates a surface composed of significant amounts of water ice (e.g. Barucci et al. 2008), as well as ammonia or an ammonia compound. A binary TNO with a known size, Orcus is also known to have a density, 1.5 ± 0.3 g/cm^3, which is intermediate between those of the small TNOs (which are typically $\leq$1), and the largest objects such as Pluto and Eris, with densities $\geq$2).

Makemake is particularly interesting because of its exceptionally strong absorption bands from methane ice on its surface (the bands are much stronger than those seen on any other icy solar system object, including Pluto) (e.g. Brown et al. 2007; Eluszkiewicz et al. 2007). The most abundant volatile on Pluto and Triton is nitrogen; while the intrinsically very weak absorption features of nitrogen have not been observed on Makemake, its presence is suggested by the shift in the wavelength of the methane ice bands (Tegler et al. 2008). *Spitzer* thermal data for Makemake (Stansberry et al. 2008) were also intriguing, showing not only that it is exceptionally large (with a diameter near 1500 km), but that the surface is probably segregated into high- and low-albedo terrains. Here we report our new *Herschel* (Pilbratt et al. 2010) SPIRE (Griffin et al. 2010) photometry of Orcus and Makemake, and *Herschel* PACS (Poglitsch et al. 2010) photometry of Makemake. We combine the results with those obtained from the earlier *Spitzer* data for these objects to form a more complete and accurate picture of their physical characteristics. Our *Herschel* TNO key programme (Müller et al. 2009) seeks to determine the properties of 139 TNOs mainly using the *Herschel* PACS instrument via photometry at 70, 100 and 160 μm. For the 15 brightest objects the programme will also obtain SPIRE photometry at 250, 350 and 500 μm. Orcus and Makemake were observed as part of the *Herschel* science demonstration phase sub-programme, which was aimed at validating the scientific useability and performance of the *Herschel* instrument observing modes. This programme included observations of 17 of our targets, PACS measurements of 7 of these targets are discussed in Paper I (Müller et al. 2010) and the lightcurve of 136108 Haumea is discussed in Paper II (Lellouch et al. 2010).

⋆ *Herschel* is an ESA space observatory with science instruments provided by European-led Principal Investigator consortia and with important participation from NASA.

Table 1. *Herschel* observing geometry for Orcus and Makemake.

Target	r [AU]	Δ [AU]	α [°]	H_V [mag]	Δ_{mag}	P [h]	Ref.
136472 Makemake	52.14	52.40	1.05	0.14 ± 0.05	0.014/0.029	7.65	1, 2
90482 Orcus	47.88	47.76	1.19	2.43 ± 0.07	0.04 ± 0.01	10.47	1, 3

Notes. r: Sun-target distance, Δ: *Herschel*-target distance, α: phase angle, H_V magnitudes, lightcurve Δ_{mag}, and the rotation period [hours], references are given for the last three columns.

References. (1) Thirouin et al. (2010); (2) Heinze & de Lahunta (2009); (3) Ortiz et al. (2006).

Table 2. Summary of PACS and SPIRE observations and relevant instrument and satellite parameters.

Target	Obs. ID	Start date & time (UT)	Dur. [s]	Bands	Mode/Param.	Rep.
136472 Makemake	1342187319	2009-11-29 22:49:02	1136	Spire 250/350/500	Large map (4′, scanA)	12
	1342187320	2009-11-29 23:08:55	1136	Spire 250/350/500	Large map (4′, scanB)	12
	1342187366	2009-11-30 18:46:38	1584	Pacs 70/160	Point-source chop/nod/dither	10
	1342187367	2009-11-30 19:14:15	1584	Pacs 100/160	Point-source chop/nod/dither	10
	1342187524	2009-12-01 18:25:54	1136	Spire 250/350/500	Large map (4′, scanA)	12
	1342187525	2009-12-01 18:45:47	1136	Spire 250/350/500	Large map (4′, scanB)	12
90482 Orcus	1342187261	2009-11-28 23:52:02	1136	Spire 250/350/500	Large map (4′, scanA)	12
	1342187262	2009-11-29 00:11:55	1136	Spire 250/350/500	Large map (4′, scanB)	12
	1342187522	2009-12-01 17:37:27	1136	Spire 250/350/500	Large map (4′, scanA)	12
	1342187523	2009-12-01 17:57:20	1136	Spire 250/350/500	Large map (4′, scanB)	12

Notes. Target name, observation identifier from the *Herschel* Science Archive (OBSID), start-date/time (UT), duration, PACS/SPIRE photometer bands (in [μm]), observing mode, repetition factor for an AB chop-nod cycle (PACS) or maps (SPIRE). The SPIRE scanA and scanB maps were repeated 1−2 days later (follow-on) to catch the object after it has moved a few beams.

2. Observations

For the purposes of planning this programme, model fluxes using typical values (geometric albedo (p_v) = 0.08, beaming factor (η) = 1.25) were generated based on estimates inherited from *Spitzer* results (Stansberry et al. 2008). This led to predictions of SPIRE 250 μm fluxes of 16 and 35 mJy for 90482 Orcus and 136472 Makemake respectively for the 2009 November/December time period.

When using *Herschel* observers must select an observing mode from a small number of astronomical observation templates (AOTs). For SPIRE the pre-flight prediction for extragalactic confusion limit was expected to be in the region of 7 mJy rms for each band (Griffin et al. 2008). Because the predicted TNO fluxes were close to these values, the chop/nod point source mode would not have produced accurate measurements of the TNO fluxes, as both additional noise, close to the TNO flux levels, would be added due to sources in the reference beam, and there would be difficulty in separating the contribution from the TNO and the background sources in the on-source beam. The SPIRE small map AOT also used chopping and nodding, so we used the SPIRE large map AOT instead, which scans the source with the telescope. The large map AOT was used with minimum scan range settings, which yielded full coverage for a 4′ × 4′ field through two cross-linked sets of scans in orthogonal directions; each set of scans consisted of 12 scans giving 24 scans in each map for each of the two positions (Table 2). A second observation was made after the source had moved a distance between 108″ and 120″, which was constrained to be >3 SPIRE long wavelength array (PLW) beam FWHM away from the position of the first observation, but still within the map region.

The SPIRE data were processed with version 2.0 of the standard data processing (build 1457) (Griffin et al. 2008) to *Herschel* level 1, calibrated scan timelines. Customised processing was then applied, which adopted the following steps. Maps were generated with the standard processing for each set of scans, this used the SPIRE standard median baseline subtraction and naive mapmaker. The four maps were then aligned to correct for differences in the telescope pointing between each scan set. These differences typically were in the range 1−2″, which is consistent with the telescope pointing error (Pilbratt et al. 2010). The pointing correction was applied to the level 1 data, and single maps at each source position combining the A and B scans were then re-generated. One map was then subtracted from the other to produce a difference map. The positive and negative source in the difference map were extracted separately with the HIPE (Ott et al. 2010) aperture photometry tool. Noise estimates were made by subdividing the observations into groups of scans, then measuring the variablity of the source flux between these groups. These sigma values are reported in Table 3. No colour-correction was applied, although this would only affect the fluxes at the 1−2% level. The absolute calibration accuracy of the SPIRE photometer is currently estimated to be within 15% (Swinyard et al. 2010). The PACS data were reduced as described in Paper I (Müller et al. 2010).

3. Thermal modelling

3.1. Orcus

We used the near-Earth asteroid thermal model (NEATM) (Harris 1998) to fit the measured MIPS and SPIRE fluxes (see Müller et al. 2010, for a fuller description). The NEATM assumes a spherical shape and the temperature distribution expected for low-thermal-inertia objects. The effects of surface roughness and thermal inertia are taken into account to first order by allowing the temperature to vary until the model continuum matches the spectral distribution of the measured data.

The NEATM temperature distribution is parameterised in terms of the dimensionless "beaming parameter". The effects of conduction and surface roughness can be approximated by

Table 3. Source fluxes obtained from SPIRE and PACS photometry plus previously derived MIPS fluxes.

Target	Instrument	λ_{ref}	FD [mJy]	Error [mJy]
Makemake	MIPS	24	0.30	0.02
	MIPS	71	14.6	2.2
	PACS	70	11.4	2.7
	PACS	100	12.0	2.8
	PACS	160	16.7	3.5
	SPIRE	250	9.5	3.1
	SPIRE	350	7.1	1.8
	SPIRE	500	<8.8	
Orcus	MIPS	24	0.33	0.03
	MIPS	71	26.6	2.2
	SPIRE	250	12.3	2.3
	SPIRE	350	6.6	1.7
	SPIRE	500	<10.7	

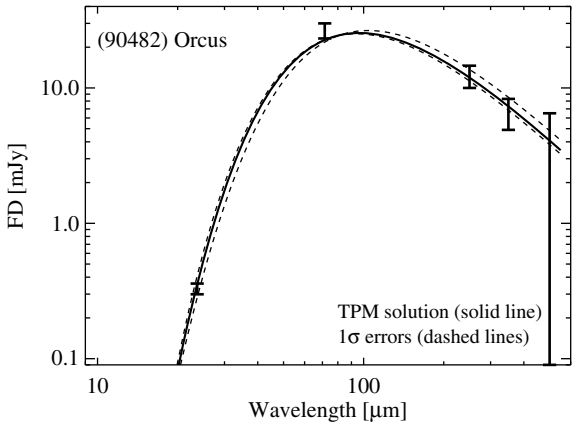

Fig. 1. TPM model of Orcus, the adopted radiometric effective diameter is $D_{\rm eff}$ = 829 km and geometric albedo p_V = 0.28 is shown by the solid line. The full albedo and diameter range is shown by the dashed lines. The 500 μm point is a 3σ upper limit and is not used in the modelling.

varying η; $\eta < 1$ corresponds to low conductivity surfaces that are rough, while $\eta > 1$ corresponds to relatively high conductivity surfaces, which are smoother. These effects can be modelled in detail with a more complicated thermophysical model (see below), but if the goal of the modelling is merely to determine the albedo (p_V) and diameter (D) of an object, the NEATM gives excellent results (Harris et al. 1998).

Uncertainties in the NEATM fit parameters were determined from a Monte-Carlo analysis. To this end, 300 sets of normally distributed flux values were generated with a random-number generator; for each wavelength, the mean of the random distribution equals the measured value, and the standard distribution equals the measured flux uncertainty. The NEATM was fitted to each of those 300 flux sets, then we determined the mean and standard distribution of each fit parameter, taken to be the overall best-fit value and its statistical uncertainty. The results are p_V = 0.25 ± 0.03, D(km) = 867 ± 57, η = 0.97 ± 0.07. This η value is slightly lower than he average η for TNOs (1.3 ± 0.4, from data in Stansberry et al. 2008), but it is consistent with the observed range. This suggests that Orcus probably has a slightly lower thermal inertia and/or rougher surface than "typical" KBOs, although this is not a very significant difference.

A thermophysical model (TPM, Lagerros 1996, 1997, 1998; Müller & Lagerros 1998) was also used to obtain radiometric properties. The TPM we used for Orcus assumes a spherical body, with the rotation period given in Table 1, and the rotation axis perpendicular to the ecliptic. The "free" parameter is the thermal inertia, $\Gamma = \sqrt{k\rho c}$, where k is the conductivity, ρ is the mass density, and c is the heat capacity per unit mass of the surface materials. Surfaces with high values of Γ tend to change temperature slowly, while those with low values of Γ (which are assumed in the NEATM/STM) approach instantaneous equilibrium with the insolation striking them.

Based on the two *Spitzer*-MIPS bands and two *Herschel*-SPIRE bands we found the best match between all observation for a very low thermal inertia below 3 J m^{-2} s$^{-0.5}$ K^{-1}. The corresponding radiometric effective diameter is $D_{\rm eff} = 829^{+119}_{-43}$ km and a geometric albedo of $p_V = 0.28^{+0.04}_{-0.06}$. The solution with the full albedo and diameter range is shown in Fig. 1.

Taking both the NEATM and TPM results into account, we adopt $p_V = 0.27^{+0.07}_{-0.05}$ and D = 850 ± 90 km as our best estimate of the albedo and diameter of Orcus. The quoted uncertainties span the range of results from these two quite different modelling approaches, and are consistent with the accuracy we expect based on previous experience for radiometric results, namely that D can be determined to no better than 10%, and p_V to no better than 20%. These uncertainties also bound those introduced by uncertainties in Orcus' absolute magnitude and lightcurve variations, although the influence of the lightcurve variation is minor, because $\Delta_{\rm mag}$ of 0.04+/−0.01 indicates that Orcus' shape is very close to a sphere and even a variation of 0.1 mag in H_V would lead to a diameter change of only 4−5% (and a change in geometric albedo of 8−10%). These values are also consistent with the D(km) = 940 ± 70 and p_V = 0.28 ± 0.04 found by Brown et al. (2010) using the *Spitzer* data only.

3.2. Makemake

As noted by Stansberry et al. (2008), Makemake is too bright at 24 microns to allow any simple thermal model to fit the spectral energy distribution (SED). This is still the case with our new *Herschel* data. As an example, we show a TPM fit to the *Herschel* and *Spitzer* data from 70−500 μm in Fig. 2. For a range of assumptions about the spin vector, TPM models with fit to these wavelengths give 1350 < D < 1510 km, and albedos 0.7 < p_V < 0.9. The model vastly under-predicts the 24 micron flux, which made us explore enhanced models.

A slightly more complex model, consisting of high-albedo and low-albedo terrains, is capable of fitting the entire SED. The surface of Makemake has large amounts of methane ice, which is volatile even at temperatures found at 52 AU from the Sun. Taking Pluto and Triton as guidance, it should be expected that the methane ice will form extensive high-albedo terrains. Additionally, the methane will sublime in areas of high-insolation, forming new deposits in darker areas. This volatile transport should expose underlying non-volatile materials (such as water ice and organics derived by photolysis from the methane). The presence of organics should cause the substrate albedo to be quite low, perhaps as dark as cometary nuclei.

Figure 2 shows an example of a two-terrain model fit to all the data. The two-terrain fit not only passes through the 24 micron *Spitzer* point, but also provides an improved fit at the PACS and SPIRE wavelengths. The family of two-terrain models that produce reasonable fits provide the following constraints. 1) For the bright terrain, 0.78 < p_V < 0.90, and the effective radius is 660 < $R_{\rm eff}$ < 715 km. 2) For the dark terrain 0.02 < p_V < 0.12, and its extent is given by 155 < $R_{\rm eff}$ < 190 km. Here $R_{\rm eff}$ is the radius of an object with the equivalent projected area as the terrain in question. Cast in another way, the dark terrain is

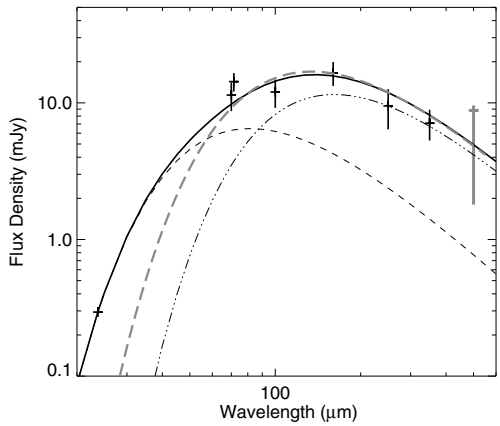

Fig. 2. Example of a two-terrain fit for the *Herschel* and *Spitzer* data for Makemake. The symbols are the measurements with error bars; the grey long-dash line is a TPM fit to the *Herschel* and *Spitzer* data from 70−500 μm, the dashed line is the emission from the low-albedo terrain; the dash-dotted line is the emission from the high albedo terrain, and the heavy solid line is the total emission for the two-terrain model. Parameters for this particular model: Terrain 1: p_V = 0.9, η = 1.9, radius = 662 km, Terrain 2: p_V = 0.04, η = 0.433, radius = 178 km, Total H_v = 0.14. *Spitzer* fluxes were normalised to the *Herschel* observer distance.

found to cover 3−7% of the surface. The range of diameters for Makemake corresponding to these radii is $1360 < D < 1480$ km, consistent with the values given above based on the TPM fit to just the long-wavelength data.

The two-terrain models used a beaming parameter for the bright terrain of $1.3 \leq \eta \leq 2.2$. The value of 1.3 is the average for TNOs, and if we assume $\eta < 1.3$ the models produce geometric albedos for Makemake ≥1. While these high albedos are not unphysical (up to values of 1.4), we know of no other planetary surface that reflective. For these two reasons we only considered values for $\eta \geq 1.3$. An η value as high as 2.2 is near the upper limit expected based on comparing thermophysical models, and mimics a surface with very high thermal inertia, which makes it a reasonable upper bound for our modeling. Volatile transport (and the accompanying transport of latent heat) can result in high values for thermal conductivity (if the tranport occurs between layers in the surface), increasing the apparent thermal inertia. Transport can also occur laterally. In cases where a thick enough atmosphere is present (e.g. Triton and Pluto) the transport of latent heat is comparable to insolation and re-radiation terms, resulting in a nearly isothermal surface (where the volatile ices exist). Methane has too low a vapor pressure for this to occur on Makemake, but there is indirect evidence (Tegler et al. 2008) in the near-IR spectrum for the presence of nitrogen. With its higher vapor pressure, nitrogen could greatly affect the temperature distribution of the high-albedo terrain.

The beaming parameter for the dark terrain is required to be quite low, in the range 0.4−0.5. These low values may require some enhancement to the normal mechanisms thought to result in "beaming". One possibility is that sunlight, scattered through and/or off nearby raised, high-albedo regions results in enhanced heating of the dark terrains. To be effective, this mechanism would require the dark regions to be comparable in size to the depth of the methane ice surrounding them. The low-amplitude visible lightcurve is not violated in this paradigm, because the dark spots would be small and probably rather evenly distributed. If the dark terrain intrinsically has such an extreme beaming parameter, it could also be distributed as a band at a constant latitude, or as a polar spot, while still being consistent with the visible lightcurve. Another possibility is that the dark terrain is actually an as-yet undiscovered satellite of Makemake. The components of most TNO binaries have very similar colours (and probably albedos), so this is not likely for a small satellite orbiting a methane-rich object such as Makemake.

4. Conclusions

The addition of *Herschel* photometry to the *Spitzer* photometry has extended the thermal SED to 350 μm and gave improved constraints for modelling. For Orcus the additional SPIRE data allowed a single well constrained model to be fitted, which shows good consistency between the *Spitzer* data and the *Herschel* data. Difficulties in fitting Makemake with a single-terrain model (suspected based on the *Spitzer* data alone) are not diminished by the new PACS and SPIRE data and a two-terrain thermal model, consisting of a limited, low-albedo terrain and an extensive, high-albedo terrain, appears to be required in order to fit the full emission spectrum. The detections were close to the instrumental limit and the measured errors are consistent with the expected instrumental noise (1.8, 1.5 and 2.2 mJy at 250, 350 and 500 μm, Griffin et al. 2010), demonstrating that SPIRE performs consistently well down to the very weakest sources it will detect. Therefore these observations have demonstrated SPIRE instrument capability and have shown that this observing strategy is the correct choice for the TNO key programme.

Acknowledgements. Part of this work was supported by the German *Deutsche Forschungsgemeinschaft, DFG* project number Ts 17/2–1. M.R. and S.P. acknowledges support from the German Deutsches Zentrum für Luft-und Raumfahrt, DLR project number 50OFO 0903. HIPE is a joint development by the *Herschel* Science Ground Segment Consortium, consisting of ESA, the NASA *Herschel* Science Centre, and the HIFI, PACS and SPIRE consortia.

References

Barucci, M. 2008, A&A, 479, L13
Brown, M. E., et al. 2007, AJ, 133, 284
Brown, M. E., et al. 2010, AJ, 139, 2700
Eluszkiewicz, J. 2007, JGRE, 11206003E
Griffin, M., et al. 2008, Proc SPIE, 7010, 70106T
Griffin, M., et al. 2008, Proc. SPIE, 7010, 70102Q
Griffin, M. J., et al. 2010, A&A, 518, L3
Harris, A. W. 1998, Icarus, 131, 291
Heinze, A. N., & de Lahunta, D. 2009, AJ, 138, 428
Lagerros, J. S. V. 1996, A&A, 310, 1011
Lagerros, J. S. V. 1997, A&A, 325, 1226
Lagerros, J. S. V. 1998, A&A, 332, 1123
Lellouch, E., et al. 2010, A&A, 518, L147
Pilbratt, G. L., et al. 2010, A&A, 518, L1
Poglitsch, A., et al. 2010, A&A, 518, L2
Müller, T. G., & Lagerros, J. S. V. 1998, A&A, 338, 340
Müller, T. G., Lellouch, E., Böhnhardt, H., et al. 2009, Earth, Moon, and Planets, 105, 209
Müller, T. G., et al. 2010, A&A, 518, L146
Ott, S. 2010, in Astronomical Data Analysis Software and Systems XIX, ed. Y. Mizumoto, K.-I. Morita, & M. Ohishi, ASP Conf. Ser., in press
Ortiz, J. L., Gutiérrez, P. J., Santos-Sanz, P., Casanova, V., & Sota, A. 2006, A&A, 447, 1131
Stansberry, J., et al. 2008, Physical Properties of Kuiper Belt and Centaur Objects: Constraints from the *Spitzer* Space Telescope, The Solar System Beyond Neptune, ed. M. A. Barucci, H. Böhnhardt, D. P. Cruikshank, & A. Morbidelli (Tucson: University of Arizona Press), 592
Swinyard, B. M., et al. 2010, A&A, 518, L4
Tegler, S. C. 2008, Icarus, 195, 844
Thirouin, A., et al. 2010, A&A, in press

[1] Space Science and Technology Department, Rutherford Appleton Laboratory, Chilton, Didcot, Oxon UK, OX11 0QX, UK
e-mail: tanya.lim@stfc.ac.uk
[2] The University of Arizona, Tucson AZ 85721, USA
[3] Max-Planck-Institut für extraterrestrische Physik, Giessenbachstrasse, 85748 Garching, Germany
[4] Université de Nice Sophia Antipolis, CNRS, Observatoire de la Côte d’Azur, Laboratoire Cassiopée B.P. 4229, 06304 Nice Cedex 4, France
[5] Observatoire de Paris, Laboratoire d’Études Spatiales et d’Instrumentation en Astrophysique (LESIA), 5 Place Jules Janssen, 92195 Meudon Cedex, France
[6] Konkoly Observatory of the Hungarian Academy of Sciences, 1525 Budapest, PO Box 67, Hungary
[7] Max-Planck-Institut für Sonnensystemforschung, Max-Planck-Straße 2, 37191 Katlenburg-Lindau, Germany
[8] Laboratoire d’Astrophysique de Marseille, CNRS & Université de Provence, 38 Rue Frédéric Joliot-Curie, 13388 Marseille Cedex 13, France
[9] Instituto de Astrofísica de Andalucía (CSIC) C/ Camino Bajo de Huétor, 50, 18008 Granada, Spain
[10] Observatoire de Paris, Laboratoire d’Études Spatiales et d’Instrumentation en Astrophysique (LESIA), University of Paris 7 “Denis Diderot”, 4 Rue Elsa Morante, 75205 Paris Cedex, France
[11] Deutsches Zentrum für Luft- und Raumfahrt, Berlin-Adlershof, Rutherfordstraße 2, 12489 Berlin-Adlershof, Germany
[12] Department of Physics and Astronomy, Science Laboratories, University of Durham, South Road, Durham, DH1 3LE, UK
[13] Newton Fellow of the Royal Society, Astrophysics Research Centre, Physics Building, Queen’s University, Belfast, County Antrim, BT7 1NN, UK
[14] Northern Arizona University, Department of Physics & Astronomy, PO Box 6010, Flagstaff, AZ 86011, USA
[15] INAF - Osservatorio Astronomico di Roma, via di Frascati, 33, 00040 Monte Porzio Catone, Italy
[16] ESO, Karl-Schwarzschild-Str. 2, 85748 Garching bei Müchen, Germany
[17] IMCCE/Observatoire de Paris, CNRS, 77 Av. Denfert-Rochereau, 75014 Paris, France
[18] *Herschel* Science Centre, European Space Astronomy Centre (ESAC), Camino bajo del Castillo, s/n, Urbanizacion Villafranca del Castillo, Villanueva de la Cañada, 28692 Madrid, Spain
[19] Universität Bern, Hochschulstrasse 4, 3012 Bern, Switzerland